ACS OMEGA

Open Access

http://pubs.acs.org/journal/acsodf

Article

Gamma Irradiation Synthesis of Sugar-Derived Carbon-Dot-Functionalized Glutathione for Hg^{2+} Detection and Antioxidant Activity

Kanokorn Wechakorn, Pacharaphon Khaopueak, Varistha Chobpattana, Natakorn Sapermsap, Sorawis Sangtawesin, and Tanagorn Sangtawesin*

Cite This: *ACS Omega* 2025, 10, 4496−4504

Read Online

ACCESS | Metrics & More | Article Recommendations

ABSTRACT: Mercury, a particularly toxic heavy metal from industrial processes, poses significant risks to both people and the environment when it accumulates to dangerous levels, damaging the liver, kidneys, and nervous system. Therefore, fluorescent organic carbon dots (CDs) were developed for detecting Hg^{2+} ions. These CDs were easily synthesized, chemically stable, biocompatible, low in toxicity, and environmentally friendly. In this work, glutathione-functionalized CDs (CDs-GSH) were produced from sugar using the EDC/NHS coupling method. Gamma irradiation induced the chemical reactions necessary to produce fluorescent CDs. CDs-GSH demonstrated significant selectivity for Hg^{2+} with an 83% reduction in fluorescence intensity. Additionally, they exhibited a phenolic content of 19.1 μg/mg GAE and strong antioxidant characteristics, with DPPH radical scavenging activity of 63% at 1.0 mg/mL. Due to their stability, selectivity, and antioxidant qualities, high-value CDs can be produced from table sugar using an environmentally friendly synthesis process, offering potential applications in sensing and antioxidant activity.

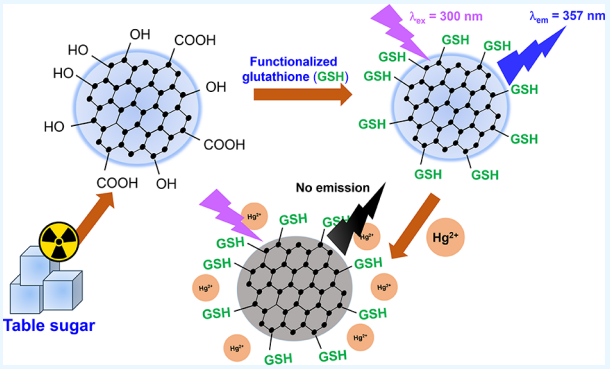

1. INTRODUCTION

Significant environmental damage has resulted from the leakage of hazardous heavy transition metals from industrial processes. These contaminants have negatively impacted human health through the respiratory system, skin contact, and food chains. Mercury, a particularly dangerous heavy metal, poses serious risks to both humans and the environment. Excessive mercury accumulation in the body can cause irreversible harm to the liver, kidneys, and nervous system.[1] When mercury is consumed, it can inhibit a large number of thiol- or selenol-containing enzymes that are essential for maintaining cellular redox equilibrium, leading to renal failure and damage to the nervous system.[2] There is strong interest in developing novel materials for the highly effective and simple detection of Hg^{2+} ions in potable water and wastewater samples. Fluorescent organic carbon dots (CDs) have many advantages, including facile synthesis, excellent chemical stability, good biocompatibility, low toxicity, environmental friendliness, and distinctive fluorescent properties, making them suitable as fluorescent probes for detecting Hg^{2+} ions.[3,4]

Table sugar, commonly known as sucrose, is a disaccharide composed of glucose and fructose molecules linked by a glycosidic bond. It was utilized due to its reasonable cost and availability, making it practical and cost-effective for large-scale production. Furthermore, sugar is an attractive precursor for the synthesis of CDs in aqueous solutions due to its high carbon and oxygen content, high solubility in water, and nontoxicity. CDs from table sugar are a type of carbon-based nanomaterial that exhibits unique optical and electronic properties, making them useful in various applications such as bioimaging, sensing, and drug delivery. For example, carbon dots from table sugar were synthesized by using microwave irradiation. These carbon dots can visibly aggregate in the presence of Pb^{2+} ions and are applied as a green reducing agent.[5,6] Doped CDs from table sugar were synthesized by using nitric, phosphoric, and sulfuric acids. Undoped CDs showed the highest UV−vis absorption, phenolic content, antioxidant activity, photostability, and biocompatibility, while heteroatom doping only improved fluorescence quantum yields.[7] CDs were successfully synthesized from xylose,

Received: August 31, 2024
Revised: January 6, 2025
Accepted: January 13, 2025
Published: January 29, 2025

glucose, sucrose, and table sugar by using a batch hydrothermal method. Among these, CDs from sucrose demonstrated the best overall efficiency, with a high quantum yield (QY) and the highest mass yield.[8] Monolayer and turbostratic bilayer N-doped graphene quantum dots from sucrose were synthesized via hydrothermal methods and exhibited sensitivity for Ag^+ ions.[9] Glutathione (GSH) contains an active thiol group that can bind with heavy metal ions, including Hg^{2+}.[10]

Gamma irradiation utilizes γ rays, a type of high-energy electromagnetic radiation capable of breaking chemical bonds and modifying the molecular structure of substances. When preparing CDs via gamma irradiation, these rays, emitted by a radioactive source, initiate chemical reactions within a carbon-containing precursor.[11] This process generates reactive species that facilitate the creation of fluorescent carbon nanoparticles. Gamma irradiation thus offers a direct and efficient approach for synthesizing CDs from carbon-rich starting materials, enabling customization of their characteristics to suit various applications in nanotechnology.[12] This synthesis method has the potential to be produced on an industrial scale, in addition to being devoid of harmful chemicals and produced at ambient temperature. For example, CDs with a high quantum yield were synthesized from water hyacinth leaves using ionizing γ radiation without requiring heat or chemical treatments.[11] Our group successfully synthesized table sugar-derived carbon dots via gamma irradiation at 25 kGy.[13] Their optical properties showed a high UV absorption peak at 271 nm and an adjustable fluorescence emission.

In this work, glutathione-functionalized CDs were synthesized from table sugar via the EDC/NHS coupling reaction. CDs were easily synthesized in one step using gamma irradiation. The chemical properties of CDs-GSH were characterized by using FTIR, XPS, DLS, TGA, and XRD methods. The photophysical properties, including UV−vis absorption, fluorescence emission, quantum yield, and photostability, were investigated. The fluorescent CDs were further evaluated for sensing Hg^{2+} ions and DPPH radical scavenging activity.

2. EXPERIMENTAL METHODS

2.1. Reagents and Instruments. No additional purification was performed on any of the analytical grade chemicals that were utilized. Pure refined sugar was purchased from a commercial store. $Pb(OAc)_2{\cdot}3H_2O$, $Zn(OAc)_2$, $Ni(OAc)_2{\cdot}4H_2O$, $Cu(OAc)_2{\cdot}H_2O$, LiCl, $Ca(OAc)_2{\cdot}H_2O$, and quinine hemisulfate monohydrate were obtained from Sigma-Aldrich. $Hg(OAc)_2$, $Pd(OAc)_2$, and $Co(OAc)_2{\cdot}4H_2O$ were purchased from Fluka. As_2O_3 was obtained from Ajax Finechem. KCl and NaCl were purchased from BDH. The 25% ammonia solution was purchased from Loba Chemie. *N*-Hydroxysuccinimide (NHS) and glutathione 98% were obtained from Thermo Scientific Chemicals. 1-(3-(Dimethylamino)propyl)-3-ethylcarbodiimide (EDC, 98%) was purchased from Alfa Aesar. 1,1-Diphenyl-2-picrylhydrazyl (DPPH), gallic acid, and Folin−Ciocalteu's reagent were purchased from Sigma-Aldrich. Sodium carbonate (Na_2CO_3) was purchased from KemAus. All experiments used deionized water ($R > 18$ MΩ cm^{-1}).

Gamma irradiation was carried out using a cobalt-60, Gamma Chamber 5000. Fourier-transform infrared (FTIR) spectra were obtained with a Thermo Scientific Nicolet is5/iD7 ATR. X-ray diffraction (XRD) profiles were recorded on a PANalytical X'Pert PRO MPD model PW 3040/60 diffractometer. High-resolution transmission electron microscopy (HRTEM) images were measured on a JEOL-3100F operated at 300 kV. The X-ray photoelectron spectrum (XPS) was acquired on a Kratos AXIS Ultra DLD instrument (Shimadzu). Zeta potentials and particle sizes were measured with a Malvern Zetasizer Ultra. UV−vis absorption spectra were collected on a Shimadzu UV-1601 UV/vis spectrometer. Fluorescence emission spectra were collected on a Hitachi F-4600 fluorescence spectrophotometer. pH values were recorded on an Ionix pH100 Benchtop pH meter. TGA analysis was explored on the thermogravimetric analyzer (TGA, TGA 4000, PerkinElmer, USA) at 30−550 °C with a heating rate of 10 °C/min under an N_2 atmosphere.

2.2. Synthesis of Carbon Dots Conjugated Glutathione (CDs-GSH). Carbon dots from table sugar were synthesized through γ radiation according to the previous protocol.[13] Sugar (20.0 g) was melted and colored brown at 100 °C. The 12.5% NH_3 solution (200 mL) was slowly added to the melted sugar and stirred continuously for 2 h. The brown sugar solution (10% w/v) was transferred into glass containers, and nitrogen gas was purged for 20 min to remove any remaining oxygen gas. The mixture was then exposed to 25 kGy of γ radiation. Subsequently, the sample was dialyzed using dialysis bags (1 kDa) in deionized water for 24 h, with the water changed every 3 h. The resulting yellow solution was freeze-dried to produce CDs.

CDs-GSH were synthesized by the coupling reaction according to the literature.[14] CDs (100 mg) were dissolved in deionized water (5 mL) and exposed to an ultrasonic bath for 30 min. A solution of EDC (800 mg) and NHS (400 mg) in deionized water (10 mL) was stirred at ambient temperature for 10 min and then added to the suspension solution of CDs with stirring for 1 h. The solution of glutathione (GSH, 200 mg) in deionized water (5 mL) was added to the resulting mixture. After stirring for 12 h, the reaction mixture was filtrated through a 0.2 μm filter and then dialyzed using dialysis bags (1 kDa) in deionized water for 24 h, with the water changed every 3 h. The resulting yellow solution was freeze-dried to produce CDs-GSH.

2.3. Determination of Fluorescence Quantum Yield. The quantum yield (Φ) of CDs-GSH was determined by comparing the slope of the sample to that of quinine sulfate monohydrate (Φ = 54%) used as the standard reference. The calculation was performed by using the following equation:

$$\Phi_x = \Phi_{ST}\frac{\text{slope}_x}{\text{slope}_{ST}}\frac{\eta_x^2}{\eta_{ST}^2}$$

The standard reference and sample were denoted by the subscripts ST and *x*, respectively. The slope was derived from the slope of the integrated absorbance and fluorescence intensity plot. The solvent's refractive index was indicated by η.

2.4. Fluorescence Experiments. Selectivity of CDs-GSH (1.0 mg/mL) toward several metal ions (1.0 mM) including LiCl, NaCl, KCl, $Cu(OAc)_2{\cdot}H_2O$, $Zn(OAc)_2$, $Pb(OAc)_2{\cdot}3H_2O$, $Zn(OAc)_2$, $Co(OAc)_2{\cdot}4H_2O$, $Mg(OAc)_2{\cdot}4H_2O$, $Hg(OAc)_2$, $Ca(OAc)_2{\cdot}H_2O$, and $Ni(OAc)_2{\cdot}4H_2O$ was investigated by an excitation wavelength of 300 nm.

Fluorescence titration of CDs-GSH with the addition of various Hg^{2+} concentrations in the range of 0−4.0 mM was elucidated by an excitation wavelength of 300 nm.

2.5. Fluorescence Lifetime Measurement. The fluorescence lifetime measurement was conducted by using a time-correlated single-photon counting (TCSPC) module (QuTAG

https://doi.org/10.1021/acsomega.4c08009
ACS Omega 2025, 10, 4496−4504

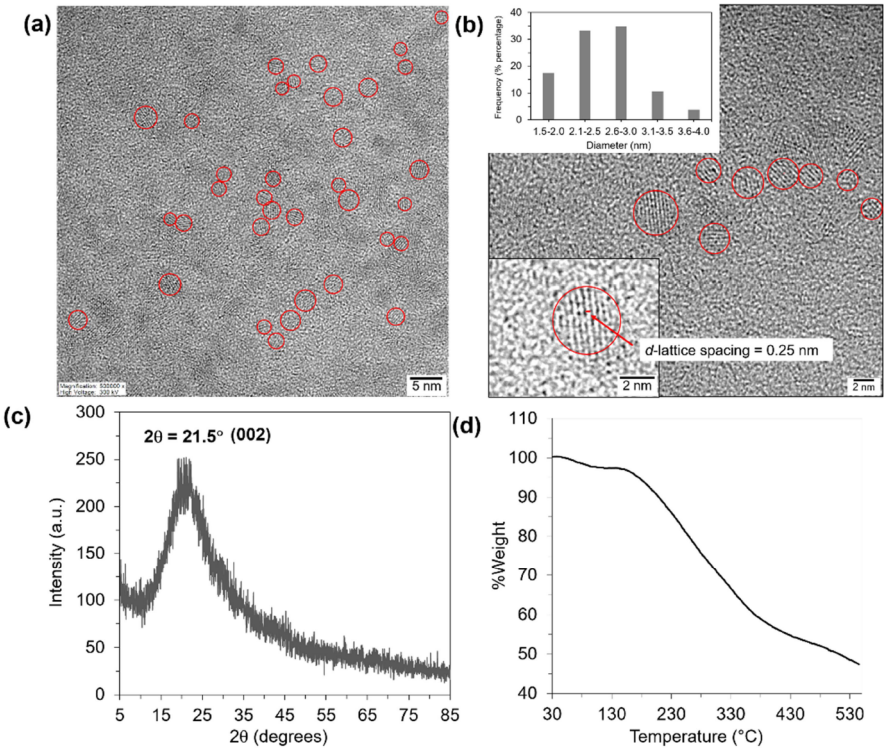

Figure 1. (a, b) HRTEM images, (c) XRD pattern, and (d) TGA thermogram of CDs-GSH (inset: size distribution diagram of CDs-GSH).

MC, QuTools) and a single-photon counter (SPCM-AQRH-43, Excelitas Technologies). A pulsed supercontinuum laser (NKT SuperK Extreme EXU-6) operating at a 78 MHz repetition rate served as the excitation source with a 405 nm excitation filter. Fluorescence emission was collected from a cuvette at a 90° angle and filtered with a 450 nm long pass (FELH0450, Thorlabs). The TCSPC timing resolution was set to 10 ps/bin, and the PL lifetime of dual exponential decay was fitted with the equation

$$\mathrm{PL}(t) = A_1 e^{-t/\tau_1} + A_2 e^{-t/\tau_2}$$

and the average lifetime was calculated from the amplitude-weighted lifetime[15]

$$\tau_{\mathrm{average}} = \frac{A_1\tau_1 + A_2\tau_2}{A_1 + A_2}$$

where τ_1 and τ_2 were the short and long decay lifetime of CDs-GSH, respectively. A_1 and A_2 were the corresponding relative weightings (% fluorescence emission) of the components, respectively. The short lifetime τ_1 was obtained by fitting the instrument response function (IRF, measured on DI water under the same conditions) to a single-exponential decay.

2.6. Evaluation of Total Phenolic Contents. The total phenolic content of CDs-GSH was elucidated by using the Folin−Ciocalteu method. The content was expressed as gallic acid equivalent (GAE) determined from a standard curve of gallic acid (0−100 μg/mL) with the equation $y = 0.0022x - 0.0045$ ($R^2 = 0.9965$). A stock solution of CDs-GSH (0.25 mg/mL, 50 μL) was added to 500 μL of a 10% Folin−Ciocalteu solution. The mixture was incubated in the dark at room temperature for 5 min. Then, 500 μL of 5% Na_2CO_3 was added, and the reaction mixture was incubated in the dark for 2 h. The absorbance of the solution at 700 nm was measured by using a UV−visible spectrophotometer.

2.7. PPH Radical Scavenging Activity. The antioxidant activity of CDs-GSH (0−1.0 mg/mL) was investigated by the DPPH radical scavenging method. A stock solution of DPPH (1.0 mM, 250 μL) in methanol (MeOH) and 50% MeOH/H_2O (250 μL) was added to the CDs-GSH solution (500 μL). The mixture was incubated in the dark at ambient temperature for 1 h. The absorbance at 550 nm was measured by using a UV−visible spectrophotometer. The percentage of DPPH inhibition by CDs-GSH was calculated using the following equation:

$$\%\mathrm{DPPH\ activity} = \left[\frac{A_{\mathrm{control}} - A_{\mathrm{sample}}}{A_{\mathrm{control}}}\right] \times 100$$

where A_{control} is the absorbance of the DPPH solution, and A_{sample} is the absorbance of the DPPH and CDs-GSH mixture.

3. RESULTS AND DISCUSSION

3.1. Synthesis of CDs-GSH. The different gamma doses, including 25, 35, and 45 kGy, did not significantly affect the preparation of sugar-derived CDs.[16] Therefore, CDs were synthesized from table sugar using γ radiation at 25 kGy. Sucrose, also known as table sugar, can be utilized as a precursor for carbon dot synthesis because of its high water solubility, reactivity, and carbon and oxygen content. The possible mechanism for CD preparation involves caramelization, which leads to hydrolysis, providing a mixture of glucose and fructose.[5] Dehydration of these hydrolysis products results in the formation of hydroxymethylfurfural (HMF).[7] The production of CDs via a bottom-up method is facilitated by reactive radical species generated by water radiolysis, such as e^-, $HO^{\cdot}$, and H_2O_2.[13] These species further reacted with HMF, leading to a combination of decomposition, polymerization, and carbonization processes to produce CDs.[17,18] The surface functional group of CDs was then functionalized with

https://doi.org/10.1021/acsomega.4c08009
ACS Omega 2025, 10, 4496−4504

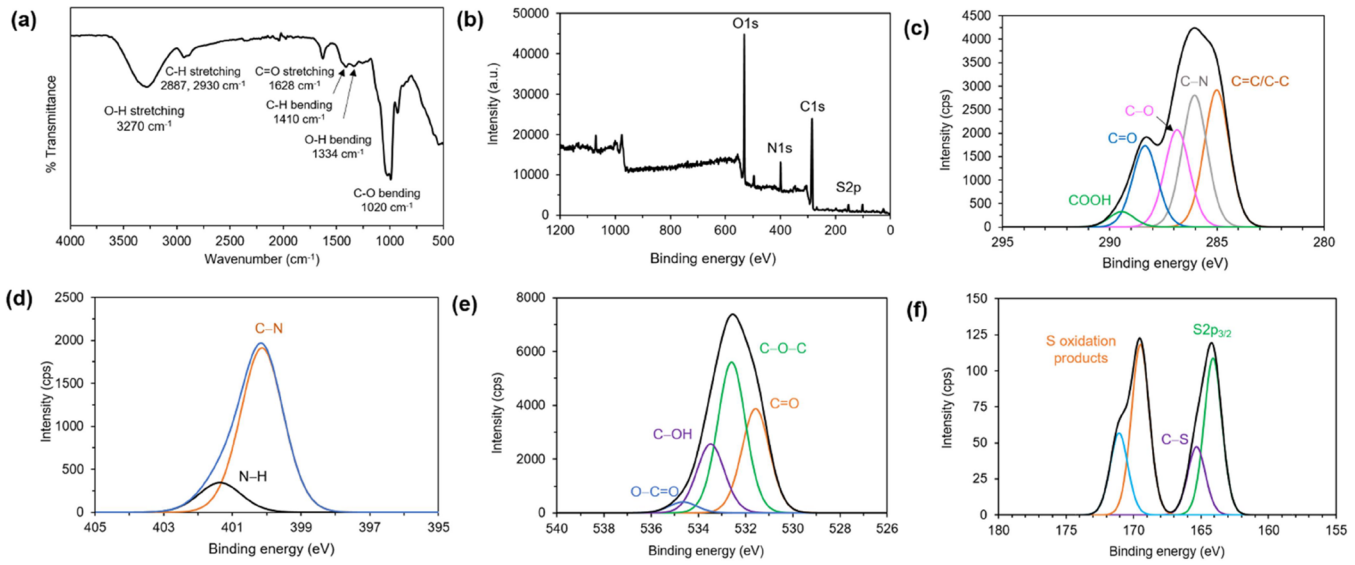

Figure 2. (a) FTIR, (b) XPS survey spectrum, and high-resolution deconvoluted spectra of (c) C 1s, (d) N 1s, (e) O 1s, and (f) S 2p of CDs-GSH.

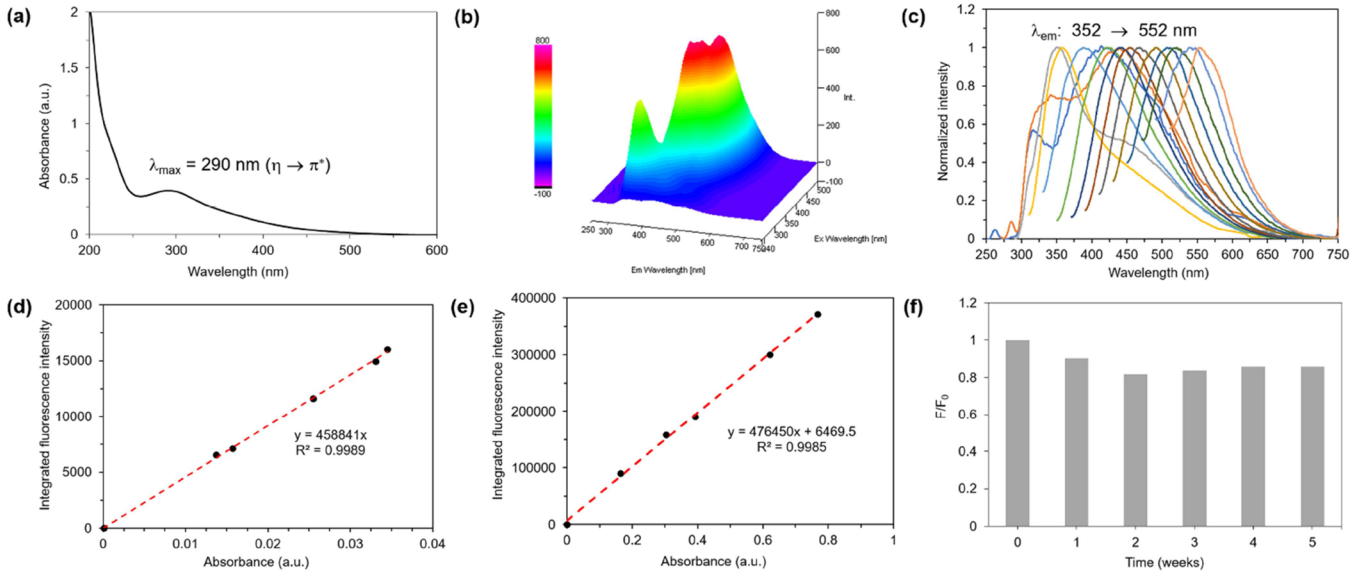

Figure 3. (a) UV−vis absorption spectra, (b) 3D fluorescence emission spectra, and (c) normalized fluorescence intensity spectra with the excitation of 240−500 nm. Quantum yield determination of (d) CDs-SH and (e) quinine sulfate monohydrate. (f) Relative fluorescence intensity of CDs-GSH (1.0 mg/mL) under visible light for 5 weeks.

glutathione through an amide coupling reaction activated by EDC/NHS.

3.2. Characterization of CDs-GSH. The morphology and size distribution of CDs-GSH were characterized by TEM images (Figure 1a,b). CDs-GSH showed uniformly spherical shapes with good dispersibility. The average diameter of CDs-GSH was found to be 2.5 nm, with a narrow size distribution from 1.8 to 4.0 nm, as confirmed by the size distribution histogram. The HRTEM image showed that the *d*-lattice spacing of CDs-GSH was 0.25 nm, corresponding to the (100) lattice plane of graphite.[19] The crystalline structure of CDs-GSH was further confirmed by an XRD analysis (Figure 1c). The XRD pattern displayed a broad peak of 2θ = 21.5°, corresponding to the (002) plane of graphite, indicative of an amorphous structure.[20]

The thermal stability of CDs-GSH was measured by using thermogravimetric (TGA) analysis (Figure 1d). The TGA thermogram displays two stages of gradual loss of weight. Due to the evaporation of water molecules and other molecules associated with weak hydrogen bonds within the CDs-GSH, an initial weight loss of 2.7% at 127 °C was observed.[21] A steady weight loss of 43.5% until 450 °C may be attributed to the degradation of organic functional groups, including glutathione in CDs-GSH as pure glutathione begins to decompose at about 200 °C.[22] The surface functional groups of CDs-GSH were characterized by using FTIR (Figure 2a). The FTIR spectrum showed several peaks associated with hydroxyl groups on the surface of CDs-GSH: at 3270 cm^{-1} for O−H stretching, at 1334 cm^{-1} for O−H bending, and at 1020 cm^{-1} for C−O bending.[11] Peaks corresponding to C−H stretching and C−H bending were observed at 2887−2930 and 1410 cm^{-1}, respectively.[23] Additionally, a C═O stretching peak of the carbonyl group appeared at 1628 cm^{-1}.[24] These results suggest that CDs-GSH exhibited sp^2/sp^3-carbon frameworks with

https://doi.org/10.1021/acsomega.4c08009
ACS Omega 2025, 10, 4496−4504

Table 1. Comparison of the Reported Carbon Dots from Disaccharide and Monosaccharide Sugars

precursors	synthesis	%QY	applications	ref.
sugar	microwave irradiation (120 °C, 3 min)	2.5%	colorimetric sensor for Pb^{2+} ions and reducing agent	5,6
sugar	hydrothermal (200 °C, 2 h)	0.032%	antioxidant and cytotoxicity	7
sugar	hydrothermal (200 °C, 6 h)			30
sugar	hydrothermal with a flow microreactor (260 °C, flow rate of 1 mL/min)	112.8%	cytotoxicity and antimicrobial drug nanocarrier	8
sucrose and ethylenediamine	hydrothermal (170 °C, 7 h)			9
glucose	caramelization and dehydration		carbon dot/polyvinyl alcohol polymer for Pb^{2+} detection	31
maltose, HCl	hydrothermal (200 °C, 3 h)		photodegradation of imipramine in wastewater	20
sugar conjugated glutathione	**gamma irradiation**	53.1 ± 1.5%	**fluorescent sensor for Hg^{2+} detection and antioxidant activity**	**this work**

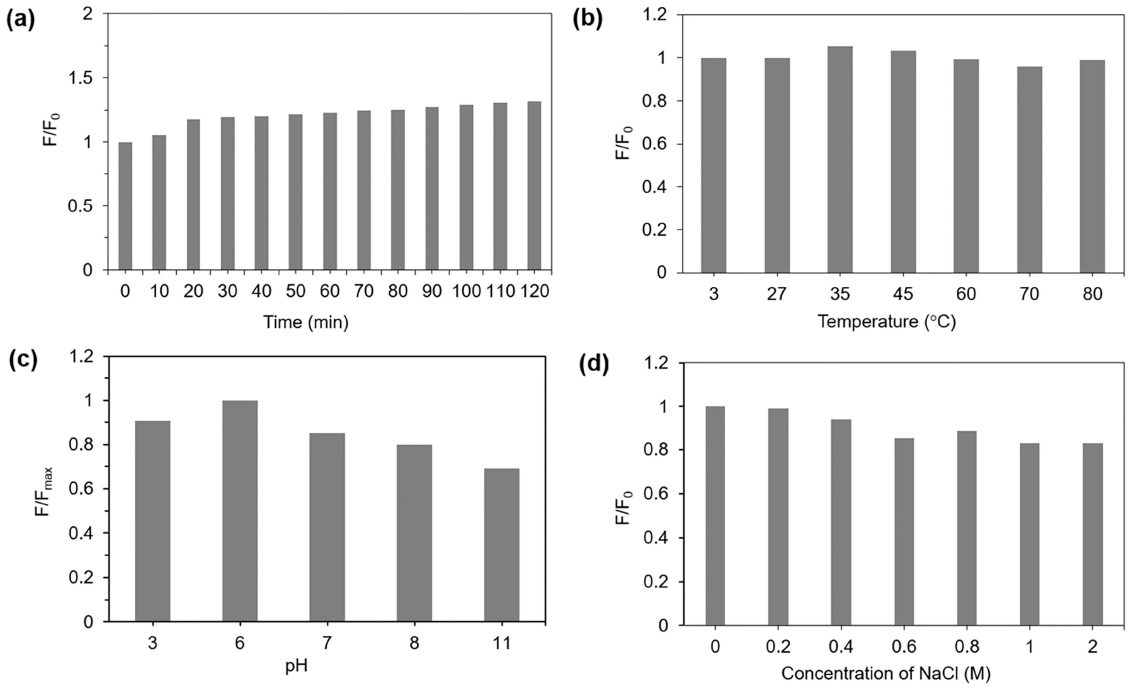

Figure 4. Relative fluorescence intensity of CDs-GSH (1.0 mg/mL) in (a) UV radiation (365 nm), (b) various temperatures, (c) buffer medium with different pH values, and (d) NaCl solution with various concentrations in the range of 0−1 M.

conjugated carbonyl and hydroxyl groups, enhancing the solubility in water.

In addition, the chemical compositions of CDs-GSH were investigated by using XPS analysis. The survey spectrum of CDs-GSH showed peaks for C 1s (285 eV, 51.6%), O 1s (532 eV, 28.9%), N 1s (400 eV, 7.3%), and S 2p (164 eV, 1.3%), indicating successful functionalization with glutathione, as evidenced by the S 2p composition (Figure 2b).[14] Furthermore, the high-resolution deconvoluted spectra for C 1s, O 1s, N 1s, and S 2p are shown in Figure 2c−f. The C 1s spectrum showed several peaks: C═C/C−C (285.0 eV), C−N (286.0 eV), C−O (286.9 eV), C═O (288.3 eV), and COOH (289.4 eV).[25] The N 1s spectrum presented two peaks at 400.1 and 401.4 eV, corresponding to C−N and N−H, respectively.[14] The O 1s spectrum exhibited peaks for C═O (531.6 eV), C−O−C (532.6 eV), C−OH (533.5 eV), and COO^- (534.6 eV).[26] The S 2p spectrum included S $2p^{3/2}$ (164.1 eV), C−S (165.3 eV), S $2p^{1/2}$ SO_4 (169.5 eV), and S $2p^{1/2}$ HSO_4 (171.1 eV).[14,27] Additionally, the CDs-GSH solution in deionized water (1.0 mg/mL) was analyzed using DLS. The zeta potential of CDs-GSH was found to be −23.6 ± 3.9 eV, likely due to the protonation of the hydroxyl group.[28]

3.3. Photophysical Property of CDs-GSH. UV−visible absorption and fluorescence emission spectroscopies were used to examine the optical characteristics of CDs-GSH in aqueous solutions, as illustrated in Figure 3. The UV−vis absorption spectra of CDs-GSH presented a strong absorption band at 290 nm, corresponding to the $\pi \rightarrow \pi^*$ transition of the conjugated C═C bonds.[18] Fluorescence emission of the CDs-GSH solution was investigated by using various excitation wavelengths ranging from 240 to 500 nm (Figure 3a−c). The maximum fluorescence intensity was observed at 357 nm with an excitation wavelength at 300 nm. Tunable fluorescence emission was observed with different excitation wavelengths (240−500 nm). A red shift in fluorescence emission was observed from 352 to 552 nm with increasing excitation wavelengths, attributed to the uniform size and emissive sites of CDs-GSH. Moreover, the quantum yield (Φ) of CDs-GSH was determined by comparing quinine sulfate monohydrate (Φ = 54%) as the standard reference (Figure 3d). The Φ of CDs-GSH was determined to be 53.1 ± 1.5%, indicating higher

https://doi.org/10.1021/acsomega.4c08009
ACS Omega 2025, 10, 4496−4504

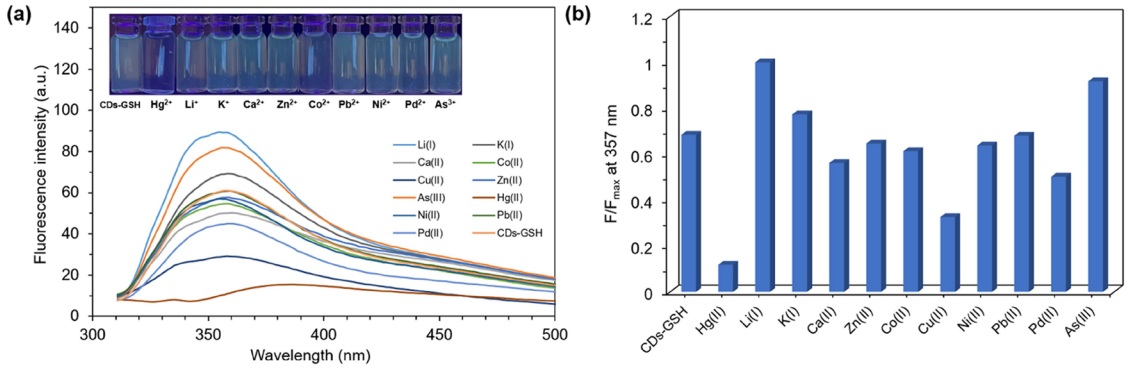

Figure 5. (a) Fluorescence emission spectra and (b) relative fluorescence intensity (F/F_{max}) at 357 nm of CDs-GSH (1.0 mg/mL) in the presence of several metal ions (1.0 mM). Inset in (a): photographs of CDs-GSH with the addition of metal ions under UV illumination.

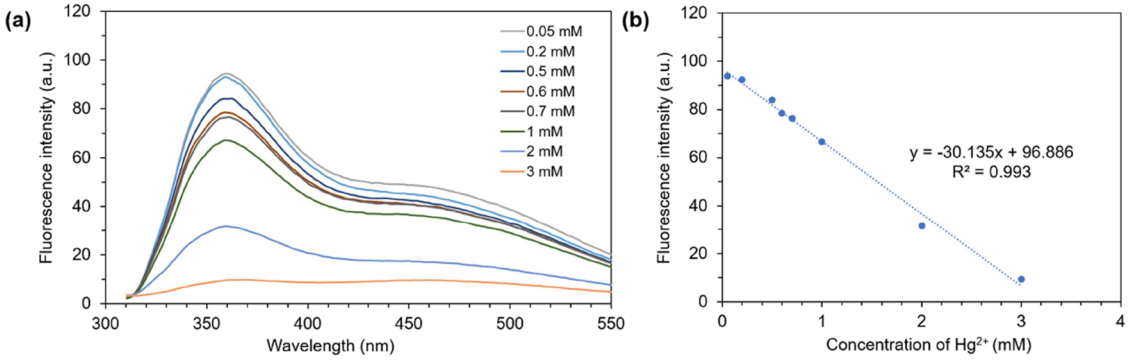

Figure 6. (a) Fluorescence titration emission spectra and (b) linear relationship curve of CDs-GSH (1.0 mg/mL) in the presence of Hg^{2+} (0.05−3.0 mM).

fluorescence emission compared to that of previous sugar-derived carbon dots, as shown in Table 1. The previous sugar-derived CDs (4% w/v) prepared via gamma irradiation showed 9.3% compared to quinine sulfate monohydrate (Φ = 54%).[16] The results suggest that the high fluorescence quantum yield of CDs-GSH may result from the edge effect of surface functionalization with glutathione. For practical applications, photostability is an essential property of optical materials. The photostability of CDs-GSH under visible light was assessed over 5 weeks in an ambient environment (Figure 3f). CDs-GSH demonstrated high stability without aggregation under visible light as the relative fluorescence intensity remained above 80%.

Photostability is an important material property that demonstrates its stability when exposed to UV radiation. The photostability of CDs-GSH was elucidated under UV illumination (365 nm) for 2 h (Figure 4a). The fluorescence emission of CDs-GSH did not decrease, suggesting that CDs-GSH showed high photostability. The thermal stability of CDs-GSH was also studied at different temperatures (Figure 4b). Fluorescence emission of CDs-GSH retained higher than 95% intensity at high temperatures, including 60−80 °C, indicating that CDs-GSH showed high thermal photostability at the high temperature. Furthermore, the stability of CDs-GSH was studied to evaluate its viability in a neutral environment. The effect of the pH on the fluorescence intensity of CDs-GSH was examined across a range of pH buffer solutions. In an acidic environment, the optical characteristics of CDs-GSH remained reasonably stable; however, in alkaline solutions, their fluorescence intensity slightly decreased (Figure 4c). This phenomenon may be attributed to the loss of surface hydroxyl functional groups in the alkaline environment.[29] The influence of the ion concentration on the stability of CDs-GSH was also tested. At various NaCl concentrations (0−1 M), the fluorescent intensity of CDs-GSH remained remarkably steady, indicating that CDs-GSH exhibit significant salt resistance and excellent fluorescence performance even in a high ion concentration environment (Figure 4d). The results demonstrate that CDs-GSH have a wide range of possible applications in natural environments due to the reliability and stability of their fluorescence properties.

3.4. Fluorescent Sensor for Hg^{2+} Detection. The selectivity of CDs-GSH toward various metal ions such as Li^+, K^+, Ca^{2+}, Co^{2+}, Cu^{2+}, Zn^{2+}, As^{3+}, Hg^{2+}, Ni^{2+}, Pb^{2+}, and Pd^{2+} was explored in deionized water (Figure 5). The fluorescence intensity of CDs-GSH significantly decreased by about 83% upon adding Hg^{2+}, while the presence of other metal ions resulted in only slight reductions. The solution of CDs-GSH displayed blue fluorescence emission under UV radiation of 365 nm. After the addition of Hg^{2+}, no fluorescence enhancement of CDs-GSH was observed except for other metal ions, as shown in Figure 5a. The strong affinity between Hg^{2+} and the sulfur atom on the surface of CDs-GSH likely contributes to its selectivity for Hg^{2+}.[14] The oxygen-containing groups on the carbon dots also bind strongly with Hg^{2+}. Therefore, the fluorescence quenching of CDs-GSH could be directed by these synergistic behaviors. However, Cu^{2+} interacts only slightly with CDs-GSH due to its binding with the glutathione on the surface of CDs.[32]

Besides, fluorescence titration spectra of CDs-GSH with different Hg^{2+} concentrations in the 0.05−3.0 mM range were

https://doi.org/10.1021/acsomega.4c08009
ACS Omega 2025, 10, 4496−4504

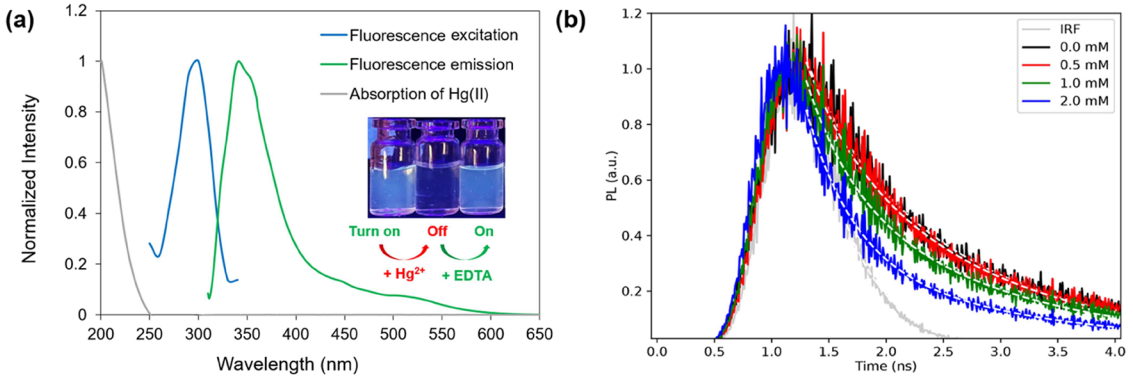

Figure 7. (a) Absorption spectra of Hg^{2+} and fluorescence spectra of CDs-GSH and (b) fluorescence decay PL spectra of CDs-GSH in the absence and presence of Hg^{2+} (0.5, 1.0, and 2.0 mM) (inset in (a): photographs under UV illumination of CDs-GSH with the addition of Hg^{2+} and EDTA, respectively).

discovered (Figure 6). Fluorescence intensities were diminished with increasing concentrations of Hg^{2+} with the linear calibration curve ($y = -30.135x + 96.886$, $R^2 = 0.993$) (Figure 6b). Besides, the limit of detection for Hg^{2+} was 0.245 mM based on the signal-to-noise ratio (S/N = 3).

3.5. Fluorescence Quenching Mechanism. The fluorescence quenching mechanism of CDs-GSH in the presence of Hg^{2+} was investigated. In the presence of Hg^{2+}, the fluorescence emission of CDs-GSH was not observed under UV illumination. The absorption spectrum of Hg^{2+} as the quencher did not overlap with fluorescence excitation and fluorescence emission of CDs-GSH. These results suggest that the inner filter effect and fluorescence resonance energy transfer (FRET) mechanism did not involve fluorescence quenching of CDs-GSH.[14] Furthermore, two primary classifications of fluorescence quenching mechanisms, dynamic and static quenching, may be distinguished by measuring the change in fluorescence lifetimes.[33] Consequently, the fluorescence quenching mechanism of CDs-GSH for Hg^{2+} binding was studied by using a fluorescence lifetime experiment (Figure 7). The fluorescence lifetime (τ) of CDs-GSH was 1.24 ns with a biexponential decay trace. After Hg^{2+} was added as the quencher, the dual exponential decay of quenched CDs-GSH was fitted with two lifetimes and average times (Table 2).

Table 2. Fluorescence Lifetime Components from the Dual Exponential Fit Decay Curves of CDs-GSH (1.0 mg/mL) in the Absence and Presence of Hg^{2+} Ions

sample	τ_1(ns)	A_1	τ_2(ns)	A_2	$\tau_{average}$(ns)
CDs-GSH	0.41	0.18	1.42	0.84	1.24
CDs-GSH + Hg^{2+} 0.5 mM	0.41	0.24	1.46	0.77	1.22
CDs-GSH + Hg^{2+} 1.0 mM	0.41	0.38	1.59	0.61	1.12
CDs-GSH + Hg^{2+} 2.0 mM	0.41	0.53	1.77	0.38	0.92

At the increasing Hg^{2+} concentrations, including 0.5, 1.0, and 2.0 mM, the average τ values were observed to be 1.22, 1.12, and 0.92 ns, respectively. The decrease in the average lifetime can be explained by the decrease of the long lifetime component A_2, along with the increasing lifetime τ_2, which is consistent with a fluorescence quenching process that involves dynamic quenching and the electron transfer process from CDs-GSH to Hg^{2+}.[28] In addition, the reversible binding of CDs-GSH with Hg^{2+} was examined using ethylenediaminetetraacetic acid (EDTA). Due to the "turn-off" fluorescence response of CDs-GSH in the presence of Hg^{2+} under UV irradiation, the addition of EDTA results in a "turn-on" fluorescence emission (Figure 7a). These results indicated that the binding mode between CDs-GSH and Hg^{2+} was a reversible process.

3.6. Antioxidant Activity. The total phenolic content of CDs-GSH was determined to be 19.1 μg/mg GAE using the Folin−Ciocalteu method. Previous literature has reported that the carbon dots containing phenolic groups exhibit DPPH radical scavenging activity.[26] Therefore, the antioxidant activity of CDs-GSH was explored by using a DPPH radical scavenging colorimetric assay (Figure 8). The DPPH free radical scavenging mechanism involves the reduction of the alcoholic DPPH solution (purple) to a nonradical form of the DPPH-H complex (yellow) in the presence of hydrogen-donating antioxidants.[34] The possible radical scavenging mechanism of CDs-GSH involves the transfer of hydrogen from the hydroxyl group on the surface functional group to DPPH$^{\cdot}$.[35] Higher concentrations of CDs-GSH showed greater DPPH inhibition activities with decreasing absorbance at 550 nm. The DPPH radical scavenging activity of CDs-GSH was found to be 63 ± 3% at the concentration of 1.0 mg/mL, better than the previously reported carbon dots.[36] These results suggest that the DPPH activities depend on the concentrations of CDs-GSH.

4. CONCLUSIONS

CDs were synthesized from table sugar (sucrose) using γ radiation due to its high water solubility, reactivity, and carbon and oxygen content. The synthesis involves caramelization, hydrolysis into glucose and fructose, and subsequent dehydration to form HMF, followed by the production of CDs. CDs were functionalized with glutathione (GSH) via an amide coupling reaction by using EDC/NHS activation. XPS analysis confirmed the successful functionalization with GSH, revealing the presence of C 1s, O 1s, N 1s, and S 2p. XRD analysis showed an amorphous structure with a broad peak at 21.5°. The optical properties included a strong absorption band and a tunable fluorescence emission. CDs-GSH exhibited a quantum yield of 53.1% and high photostability. They demonstrated significant selectivity for Hg^{2+}, reducing fluorescence intensity by 83%. Furthermore, according to the signal-to-noise ratio (S/N = 3), the limit of detection for Hg^{2+} was 0.245 mM. CDs-GSH also showed notable total phenolic content and DPPH radical scavenging activity. This study highlights a green synthesis method for transforming table

https://doi.org/10.1021/acsomega.4c08009
ACS Omega 2025, 10, 4496−4504

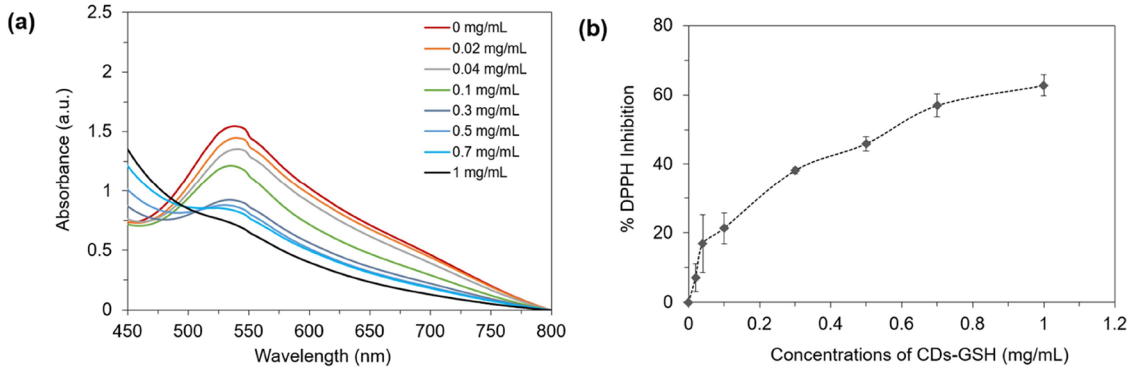

Figure 8. (a) Absorption spectra and (b) % DPPH inhibition plot of CDs-GSH (0−1.0 mg/mL).

sugar into high-value CDs, with potential applications in electronics, catalysis, and sensing due to their stability, selectivity, and antioxidant properties.

AUTHOR INFORMATION

Corresponding Author

Tanagorn Sangtawesin − *Thailand Institute of Nuclear Technology (Public Organization), Nakorn Nayok 26120, Thailand;* orcid.org/0000-0003-2377-8969; Email: tanagorn@tint.or.th

Authors

Kanokorn Wechakorn − *Department of Chemistry, Faculty of Science and Technology and Advanced Photochemical and Electrochemical Materials Research Unit, Faculty of Science and Technology, Rajamangala University of Technology Thanyaburi, Pathum Thani 12110, Thailand;* orcid.org/0000-0001-6985-8214

Pacharaphon Khaopueak − *Department of Chemistry, Faculty of Science and Technology, Rajamangala University of Technology Thanyaburi, Pathum Thani 12110, Thailand*

Varistha Chobpattana − *Department of Materials and Metallurgical Engineering, Faculty of Engineering, Rajamangala University of Technology Thanyaburi, Pathum Thani 12110, Thailand*

Natakorn Sapermsap − *School of Physics, Institute of Science, Suranaree University of Technology, Nakhon Ratchasima 30000, Thailand*

Sorawis Sangtawesin − *School of Physics, Institute of Science, Suranaree University of Technology, Nakhon Ratchasima 30000, Thailand; Center of Excellence in Advanced Functional Materials, Suranaree University of Technology, Nakhon Ratchasima 30000, Thailand*

Complete contact information is available at: https://pubs.acs.org/10.1021/acsomega.4c08009

Author Contributions

K.W.: conceptualization, methodology, visualization, resources, writing—original draft, review, and editing, project administration, funding acquisition. P.K.: investigation, visualization. V.C.: investigation, writing—review and editing. N.S.: investigation, methodology, writing—review and editing. S.S.: investigation, methodology, visualization, writing—review and editing. T.S.: conceptualization, methodology, resources, writing—review and editing, funding acquisition.

Notes

The authors declare no competing financial interest.

ACKNOWLEDGMENTS

This work was supported by the TINT to University program, Thailand Science Research and Innovation (TSRI), National Science, Research and Innovation Fund (NSRF) (project number 197237), and IAEA Coordinated Research Project (F22081). N.S. and S.S. acknowledge funding support from the NSRF via the Management Unit for Human Resources & Institutional Development, Research and Innovation (grant numbers B39G680007 and B13F670064). The authors thank RMUTT Central Lab, Institute of Research and Development, Rajamangala University of Technology Thanyaburi, and Thailand Institute of Nuclear Technology (Public Organization) for facility support.

REFERENCES

(1) Labeb, M.; Sakr, A.-H.; Soliman, M.; Abdel-Fattah, T. M.; Ebrahim, S. Effect of capping agent on selectivity and sensitivity of CdTe quantum dots optical sensor for detection of mercury ions. *Opt. Mater.* **2018**, *79*, 331−335.

(2) Wang, C.; Wang, Y.; Shi, H.; Yan, Y.; Liu, E.; Hu, X.; Fan, J. A strong blue fluorescent nanoprobe for highly sensitive and selective detection of mercury(II) based on sulfur doped carbon quantum dots. *Mater. Chem. Phys.* **2019**, *232*, 145−151.

(3) Sharma, V.; Tiwari, P.; Mobin, S. M. Sustainable carbon-dots: recent advances in green carbon dots for sensing and bioimaging. *J. Mater. Chem. B* **2017**, *5* (45), 8904−8924.

(4) Semeniuk, M.; Yi, Z.; Poursorkhabi, V.; Tjong, J.; Jaffer, S.; Lu, Z.-H.; Sain, M. Future Perspectives and Review on Organic Carbon Dots in Electronic Applications. *ACS Nano* **2019**, *13* (6), 6224−6255.

(5) Ansi, V. A.; Renuka, N. K. Table sugar derived Carbon dot−a naked eye sensor for toxic Pb2+ ions. *Sens. Actuators, B* **2018**, *264*, 67−75.

(6) Ansi, V. A.; Sreelakshmi, P.; Poovathinthodiyil, R.; Renuka, N. K. Table sugar derived carbon dot—A promising green reducing agent. *Mater. Res. Bull.* **2021**, *139*, No. 111284.

(7) Supjaroenpisan, M.; Hanchaina, R.; Kangsamaksin, T.; Paoprasert, P. Effects of Heteroatom Doping of Carbon Dots from Sugar on Optical Properties, Phenolic Content, Antioxidant Activity, Photostability, and Cytotoxicity. *ChemistrySelect* **2021**, *6* (15), 3597−3604.

(8) Supajaruwong, S.; Porahong, S.; Wibowo, A.; Yu, Y. S.; Khan, M. J.; Pongchaikul, P.; Posoknistakul, P.; Laosiripojana, N.; Wu, K. C. W.; Sakdaronnarong, C. Scaling-up of carbon dots hydrothermal synthesis from sugars in a continuous flow microreactor system for biomedical application as in vitro antimicrobial drug nanocarrier. *Sci. Technol. Adv. Mater.* **2023**, *24* (1), No. 2260298.

(9) Ruammaitree, A.; Praphanwong, K.; Taiphol, A. Facile one-step hydrothermal synthesis of monolayer and turbostratic bilayer n-doped graphene quantum dots using sucrose as a carbon source. *RSC Adv.* **2023**, *13* (34), 23700−23707.

https://doi.org/10.1021/acsomega.4c08009
ACS Omega 2025, 10, 4496−4504

(10) Zhong, Y.; Deng, C.; He, Y.; Ge, Y.; Song, G. Glutathione-protected silver nanoclusters for sensing trace-level Hg2+ in a wide pH range. *Analytical Methods* **2015**, *7* (4), 1558−1562.
(11) Wechakorn, K.; Chutimasakul, T.; Duangmanee, T.; Weerasuk, B.; Laksee, S.; Kaeopookum, P.; Seesuea, C.; Sangtawesin, T. Gamma-irradiation assisted green synthesis of water hyacinth-derived carbon dots for enhanced photoselective film applications. *Carbon Resour. Convers.* **2025**, *8*, No. 100240.
(12) Kwamman, T.; Chutimasakul, T.; Sangangam, P.; Puengposop, N.; Wechakorn, K. Poly(vinyl)alcohol film composited with carbon dots from water hyacinth stalks based on gamma irradiation for the UV blocking film. *J. Met. Mater. Miner.* **2021**, *31* (4), 123−128.
(13) Wechakorn, K.; Utapong, T.; Chutimasakul, T.; Sirisit, N.; Kwamman, T. Optical properties of carbon dots derived from table sugar via gamma irradiation. *Journal of Physics: Conference Series* **2023**, *2431* (1), No. 012014.
(14) Seesuea, C.; Sangtawesin, T.; Thangsunan, P.; Wechakorn, K. Facile Green Gamma Irradiation of Water Hyacinth Derived-Fluorescent Carbon Dots Functionalized Thiol Moiety for Metal Ion Detection. *J. Fluoresc.* **2023**, *34*, 1761−1773.
(15) Saiyasombat, W.; Muangsopa, P.; Khrootkaew, T.; Chansaenpak, K.; Pinyou, P.; Sapermsap, N.; Sangtawesin, S.; Kamkaew, A. Halogenated BOIMPYs and Their Efficiency in Photodynamic Therapy. *ChemPhotoChem* **2024**, *8* (10), No. e202400109.
(16) Wechakorn, K.; Utapong, T.; Chutimasakul, T.; Sirisit, N.; Kwamman, T. In *Optical properties of carbon dots derived from table sugar via gamma irradiation*. *J. Phys.: Conf. Ser.* **2023**, *2431*, No. 012014.
(17) Gude, V.; Das, A.; Chatterjee, T.; Mandal, P. K. Molecular origin of photoluminescence of carbon dots: aggregation-induced orange-red emission. *Phys. Chem. Chem. Phys.* **2016**, *18* (40), 28274−28280.
(18) Rigodanza, F.; Burian, M.; Arcudi, F.; Đorđević, L.; Amenitsch, H.; Prato, M. Snapshots into carbon dots formation through a combined spectroscopic approach. *Nat. Commun.* **2021**, *12* (1), 2640.
(19) Surendran, P.; Lakshmanan, A.; Vinitha, G.; Ramalingam, G.; Rameshkumar, P. Facile preparation of high fluorescent carbon quantum dots from orange waste peels for nonlinear optical applications. *Luminescence* **2020**, *35* (2), 196−202.
(20) Hatefi, R.; Mashinchian-Moradi, A.; Younesi, H.; Nojavan, S. Graphene quantum dots based on maltose as a high yield photocatalyst for efficient photodegradation of imipramine in wastewater samples. *Journal of Environmental Health Science and Engineering* **2020**, *18* (2), 1531−1540.
(21) Mehta, V. N.; Jha, S.; Singhal, R. K.; Kailasa, S. K. Preparation of multicolor emitting carbon dots for HeLa cell imaging. *New J. Chem.* **2014**, *38* (12), 6152−6160.
(22) Malik, L. A.; Bashir, A.; Manzoor, T.; Pandith, A. H. Microwave-assisted synthesis of glutathione-coated hollow zinc oxide for the removal of heavy metal ions from aqueous systems. *RSC Adv.* **2019**, *9* (28), 15976−15985.
(23) Klongklaw, K.; Phiromkaew, B.; Kiatsuksri, P.; Kankit, B.; Anantachaisilp, S.; Wechakorn, K. Green one-step synthesis of mushroom-derived carbon dots as fluorescent sensors for Fe3+ detection. *RSC Adv.* **2023**, *13* (44), 30869−30875.
(24) Cai, L.; Fu, Z.; Cui, F. Synthesis of Carbon Dots and their Application as Turn Off−On Fluorescent Sensor for Mercury (II) and Glutathione. *J. Fluoresc.* **2020**, *30* (1), 11−20.
(25) Huang, Y.-L.; Tien, H.-W.; Ma, C.-C. M.; Yang, S.-Y.; Wu, S.-Y.; Liu, H.-Y.; Mai, Y.-W. Effect of extended polymer chains on properties of transparent graphene nanosheets conductive film. *J. Mater. Chem.* **2011**, *21* (45), 18236−18241.
(26) Seesuea, C.; Sansenya, S.; Thangsunan, P.; Wechakorn, K. Green synthesis of elephant manure-derived carbon dots and multifunctional applications: Metal sensing, antioxidant, and rice plant promotion. *Sustainable Materials and Technologies* **2024**, *39*, No. e00786.
(27) Tresintsi, S.; Simeonidis, K.; Pliatsikas, N.; Vourlias, G.; Patsalas, P.; Mitrakas, M. The role of SO42−surface distribution in arsenic removal by iron oxy-hydroxides. *J. Solid State Chem.* **2014**, *213*, 145−151.
(28) Sachdev, A.; Gopinath, P. Green synthesis of multifunctional carbon dots from coriander leaves and their potential application as antioxidants, sensors and bioimaging agents. *Analyst* **2015**, *140* (12), 4260−4269.
(29) Wang, G.; Zhang, S.; Cui, J.; Gao, W.; Rong, X.; Lu, Y.; Gao, C. Preparation of nitrogen-doped carbon quantum dots from chelating agent and used as fluorescent probes for accurate detection of ClO− and Cr(VI). *Anal. Chim. Acta* **2022**, *1195*, No. 339478.
(30) Papaioannou, N.; Marinovic, A.; Yoshizawa, N.; Goode, A. E.; Fay, M.; Khlobystov, A.; Titirici, M.-M.; Sapelkin, A. Structure and solvents effects on the optical properties of sugar-derived carbon nanodots. *Sci. Rep.* **2018**, *8* (1), 6559.
(31) Ravi, S.; Jayaraj, M. K. Luminescent polymer composite made of glucose derived carbon dots/polyvinyl alcohol for the sensitive detection of Pb2+ in water. *J. Photochem. Photobiol., A* **2024**, *451*, No. 115523.
(32) Hu, Z.; Long, W.; Liu, T.; Guan, Y.; Lei, G.; Suo, Y.; Jia, M.; He, J.; Chen, H.; She, Y.; Fu, H. A sensitive fluorescence sensor based on a glutathione modified quantum dot for visual detection of copper ions in real samples. *Spectrochimica Acta Part A: Molecular and Biomolecular Spectroscopy* **2023**, *294*, No. 122517.
(33) Zhao, X.; Liao, S.; Wang, L.; Liu, Q.; Chen, X. Facile green and one-pot synthesis of purple perilla derived carbon quantum dot as a fluorescent sensor for silver ion. *Talanta* **2019**, *201*, 1−8.
(34) Qu, X.; Gao, C.; Fu, L.; Chu, Y.; Wang, J.-H.; Qiu, H.; Chen, J. Positively Charged Carbon Dots with Antibacterial and Antioxidant Dual Activities for Promoting Infected Wound Healing. *ACS Appl. Mater. Interfaces* **2023**, *15* (15), 18608−18619.
(35) Innocenzi, P.; Stagi, L. Carbon dots as oxidant-antioxidant nanomaterials, understanding the structure-properties relationship. *A critical review. Nano Today* **2023**, *50*, No. 101837.
(36) Rajamanikandan, S.; Biruntha, M.; Ramalingam, G. Blue Emissive Carbon Quantum Dots (CQDs) from Bio-waste Peels and Its Antioxidant Activity. *Journal of Cluster Science* **2022**, *33* (3), 1045−1053.

https://doi.org/10.1021/acsomega.4c08009
ACS Omega 2025, 10, 4496−4504